and solve Eq. (A–9) under the assumption that all other amplitudes $A(s)$ may be dropped from the right-hand side. We then find for states other than θ_1 and θ_2

$$A(s)=\frac{2^{-\frac{1}{2}}}{i\hbar}\left\{V_{s1}\frac{\exp[(i\omega_{s1}-\frac{1}{2}\gamma_1)t]-1}{i\omega_{s1}-\frac{1}{2}\gamma_1}\right.$$
$$\left.+V_{s2}\frac{\exp[(i\omega_{s2}-\frac{1}{2}\gamma_2)t]-1}{i\omega_{s2}-\frac{1}{2}\gamma_2}\right\}. \quad (A–11)$$

The probability $P(s)$ for finding the system in state s is obtained by integrating $|A(s)|^2$ over all values of the energy E_s. Under the usual assumption that V_{si} is a well-behaved analytic function of ω_{si} in the complex

plane we obtain

$$P(s)=\frac{a_{s1}{}^2}{2\lambda_1}[1-\exp(-\lambda_1 t)]+\frac{a_{s2}{}^2}{2\lambda_2}[1-\exp(-\lambda_2 t)]$$
$$+a_{s1}a_{s2}\,\mathrm{Re}\frac{1-\exp[-(\gamma_1+\gamma_2{}^*)t/2]}{\gamma_1+\gamma_2{}^*}, \quad (A–12)$$

where λ_i is the real part of γ_i and a_{si} is proportional to V_{si}.

Taking the time derivative of $P(s)$, we find for the rate of decay into modes s the expression given by Eq. (8), where $\Delta\omega$ is the imaginary part of $(\gamma_1+\gamma_2{}^*)/2$ and may be interpreted as a mass difference between the θ_1 and θ_2 particles.

Neutral Pion Production in Deuterium and Hydrogen: Ratios*

J. C. KECK,† A. V. TOLLESTRUP, AND H. H. BINGHAM
California Institute of Technology, Pasadena, California
(Received May 21, 1956)

Neutral photopion production in deuterium and hydrogen has been studied by counting the decay photons singly. Pure gas targets were used. The photon counter consisted of three counters, the first in anticoincidence and the second and third in coincidence. The photon counting rate was obtained by taking the difference between the counting rates with a Pb converter alternately behind and in front of the anticoincidence counter. Data were obtained for 300-, 400-, and 500-Mev bremsstrahlung at laboratory angles of 30, 73, and 140°. An attempt to apply the photon-difference method was only moderately successful owing to poor control of the bremsstrahlung end point and the unfavorable shape of the neutral pion excitation curve. At 73° and 140° the data are consistent with a constant value of 0.90 per nucleon for the deuterium-to-hydrogen neutral photopion production ratio. At 30° and 300 Mev there is some evidence for a larger ratio, which points to constructive interference between production on the proton and neutron in the deuteron. The data are consistent with the predictions of the "symmetrical theory" concerning the coupling of neutral pions to nucleons and with Watson's phenomenological theory of photopion production.

I. INTRODUCTION

THE four basic reactions involving photopion production on nucleons are

$$\gamma+p\rightarrow n+\pi^+, \qquad (a)$$
$$\gamma+p\rightarrow p+\pi^0\rightarrow p+2\gamma, \qquad (b)$$
$$\gamma+n\rightarrow n+\pi^0\rightarrow n+2\gamma, \qquad (c)$$
$$\gamma+n\rightarrow p+\pi^-. \qquad (d)$$

Of these, (a) and (b) are directly accessible for experimental study and considerable information has been accumulated concerning their cross sections.[1,2] The

cross sections for (c) and (d), however, can only be inferred from studies made on complex nuclei, the most suitable of which is the deuteron. Because of its loose binding, the neutron in the deuteron can be considered "almost free" for high-energy interactions. In addition, one hopes that the simple structure of the deuteron may make it possible to correct for the effects of binding and thus deduce fairly precise information about the elementary interactions with the neutron. Quite precise studies of the π^-/π^+ ratio in deuterium[3] have also been made which give information about reaction (d). This information has been reasonably well interpreted in conjunction with that on the first two processes by the phenomenological theory of Watson.[4] The theory then leads to the unique prediction that the cross sections for photopion production on neutron and proton should be

---

[1] Experiments on positive photopion production in hydrogen are reviewed in papers on this subject by Walker, Teasdale, Peterson, and Vette, Phys. Rev. 99, 210 (1955) and Tollestrup, Keck, and Worlock, Phys. Rev. 99, 220 (1950).
[2] Experiments on neutral photopion production are reviewed in papers on the subject by Goldschmidt-Clermont, Osborne, and M. Scott, Phys. Rev. 97, 188 (1955) and by D. C. Oakley and R. L. Walker, Phys. Rev. 97, 1283 (1955).
[3] Sands, Teasdale, and Walker, Phys. Rev. 95, 592 (1954).
[4] Watson, Keck, Tollestrup, and Walker, Phys. Rev. 101, 1159 (1956).

approximately equal. As always with unique predictions, an experimental check is high desirable.

Experimentally the reaction $\gamma+n\rightarrow n+\pi^0$ is the most difficult of the four to detect since all the products are neutral. The technique of counting the recoil protons[2] which has given the best information on the mirror process $\gamma+p\rightarrow p+\pi^0$ is not readily applicable since we have no suitable energy-sensitive neutron detector of reasonably large and well-known efficiency. The problem has, therefore, been attacked by the alternative scheme of counting the photons from the decay of the neutral pion. Here one has the choice of counting the decay photons in coincidence or singly. The former technique was first used by Steinberger, Panofsky, and Steller[5] in an experiment proving the existence and mode of decay of neutral pions. It has been used to study neutral meson production in deuterium and hydrogen by Andre.[6] The latter technique was introduced by Cocconi and Silverman[7] who used it also in studies on deuterium and hydrogen. These experiments were performed with 300-Mev bremsstrahlung and gave a deuterium-to-hydrogen ratio for neutral pion production of about 2.

In the present experiment we have used the technique of counting only a single photon. One objective of the experiment was to improve the precision of the deuterium-to-hydrogen neutral pion ratios and extend them to higher energies. The present paper reports the results of this work. A second objective was to extend the range over which the angular distribution for neutral photopion production has been measured to more forward angles. These data are still being reduced.

In Secs. II and III of this paper the experimental apparatus and procedure are discussed. The results are given in Sec. IV. Section V contains a discussion of the results and a comparison with other experiments.

II. EXPERIMENTAL APPARATUS

The experimental arrangement used to detect secondary photons produced by high-energy bremsstrahlung in deuterium and hydrogen is shown in Fig. 1. The bremsstrahlung beam from the California Institute of Technology 500-Mev synchrotron was collimated to a diameter of $1\frac{1}{2}$ in. at the external target by a primary collimator at the exit port. Two secondary collimators were employed to reduce the background of scattered radiation from the primary collimator. The beam intensity was monitored by an ionization chamber having 1-in. copper walls located behind the target. For that portion of the experiment covered in this report on deuterium-to-hydrogen ratios, the absolute monitor calibration was immaterial. However, in order to use the photon difference method, one must know how the calibration varies with the bremsstrahlung end point.

This was determined for a 300- and 500-Mev bremsstrahlung by the shower curve technique.[8] Interpolation between these points was accomplished by assuming the charge collected on the monitor to be proportional to the total beam energy times a correction factor $(1-0.6E^2)$, where E is the bremsstrahlung end point in Bev. The form of this factor was suggested by inspection of the Monte Carlo shower curves of Wilson.[9]

The targets were hydrogen and deuterium gas at approximately 2000 psi and liquid nitrogen temperature. Mass spectrographic analyses showed the hydrogen to be pure to 0.04% and the deuterium to be contaminated by 1% hydrogen but free of other contaminants to 0.04%. The vessel containing the gas was 17 in. long and 2-in. in diameter and had 30-mil steel walls. Thermal insulation was provided by $1\frac{1}{2}$ in. of Styrofoam. The temperature and pressure of the gas were monitored and used to determine its specific volume from the equation of state.[10]

The photon counter consisted of three liquid scintillators, the first in anticoincidence and the second and third in coincidence. An aluminum absorber was inserted between counters 2 and 3 to reduce the background of coincidences due to low-energy events. The photon counting rate was deduced from the difference
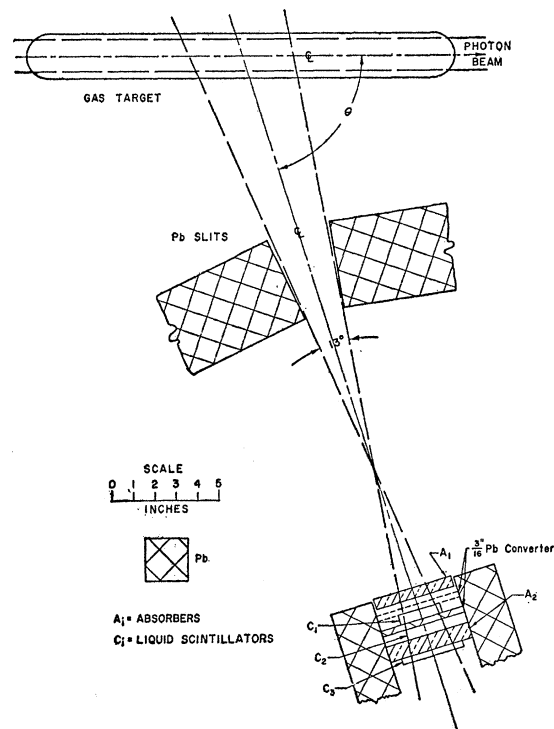

FIG. 1. Plan view of experimental arrangement.

[5] Steinberger, Panofsky, and Steller, Phys. Rev. 78, 802 (1950).
[6] Calvin G. Andre, University of California Radiation Laboratory Report UCRL-2425, 1953 (unpublished).
[7] G. Cocconi and A. Silverman, Phys. Rev. 88, 1230 (1952).

[8] Method of Blocker, Kenny, and Panofsky, Phys. Rev. 79, 419 (1950).
[9] R. R. Wilson, Phys. Rev. 86, 261 (1952).
[10] Johnston, Bezman, Rubin, Swanson, Corak, and Rifkin, Atomic Energy Commission Report MDDC-850 (unpublished).

TABLE I. Data for counter telescope. Columns 1, 2, and 3 give the heights, widths, and thicknesses of the counters, converter, and absorbers used in the experiment. The counter dimensions are those of the active volume; the counter walls were $\frac{1}{16}$-in. Lucite. Columns 4, 5, 6, 7, and 8 give the thicknesses in g/cm², radiation lengths, geometric mean free paths, and energy units for electrons and protons. Column 9 gives the critical energy of the material. X_0 and λ_g are radiation length and geometric mean free paths respectively.

	1 h in.	2 ω in.	3 t in.	4 t' g/cm²	5 t'/X_0	6 t'/λ_g	7 E_e Mev	8 E_p Mev	9 ϵ Mev
Counter 1	3.25	2.09	0.50	1.2	0.021	0.021	2.5	40	147
Counter 2	3.00	1.75	0.50	1.2	0.021	0.021	2.5	40	147
Counter 3	3.56	2.62	0.25	0.6	0.010	0.011	1.3	24	147
Lucite wall	...	...	0.06	0.2	0.003	0.003	0.4	...	147
Pb converter	4	4	0.19	5.3	0.89	0.032	6.2	...	7
Al absorber 2	4	4	0.75	5.2	0.21	0.063	8.6	69	52
Al absorber 2	4	4	2	13.7	0.52	0.161	22.8	130	52
Al absorber 1	8	4	1	6.9	0.26	0.081	11.4	...	52
CH₂ absorber 1	8	4	6	13.7	0.24	0.25	30.5	...	154

in the counting rate with a $\frac{3}{16}$-in. lead converter between counters 1 and 2 and in front of counter 1. This method of measuring the "In-minus-Front" difference has the advantage over the conventional "In-minus-Out" method in that is leaves the flux of particles incident on the two rear coincidence counters essentially unchanged and so results in a more accurate subtraction of backgrounds and accidentals. An aluminum or paraffin absorber was used to shield the counters from a high background of low-energy electrons. Some numerical information which is useful in estimating the performance of the telescope is given in Table I. This includes the dimensions of the counters, converter, and various absorbers used and their thicknesses in g/cm², radiation lengths, geometric mean free paths, and energy units for electrons and protons. Detailed consideration of the counting technique will be given later.

The angle of observation and solid angle of acceptance were determined by counter 2 and a lead aperture in the forward shielding. The sides of this aperature were tapered so that they could not be seen by the counters. This was done in the belief that it would be easier to correct for penetration of the rear edges than for scattering off the faces. In addition, no shielding was used in any location from which particles originating in the beam could be scattered into the counters.

Since we hoped to obtain statistical accuracies of one percent or better, considerable thought was given to the stability and reliability over a period of weeks of the electronic recording equipment. The system employed is shown by the block diagram in Fig. 2. The liquid scintillators were viewed by RCA 5819 photomultipliers having independent voltage supplies with a long-time regulation and reset accuracy of $\pm 0.1\%$. Positive pulses from the last dynode of each multiplier were clipped with a 1 meter stub and fed through 200-ohm cables to a 200-Mc delay line amplifier and inverter. Two fold coincidences and delayed coincidences were then formed between counters 1 and 2 and counters 2 and 3 by using simple Garwin circuits[11] employing

[11] R. L. Garwin, Rev. Sci. Instr. 24, 618 (1953).

6AH6's. These circuits have been found reliable in operation, have no dead-time, and have high input impedance which enables them to be used in parallel. The output of the coincidence circuits was amplified and fed via 6BN6 discriminators to a slow veto unit which formed the combinations: $-(1+2)+(2+3) \equiv (-1+2+3) \equiv T, (1+2)+(2+3^*) \equiv (-1+2+3^*) \equiv A$ and $T^* - (1+2) \equiv D$. The asterisk denotes a delayed coincidence. These rates, which were designated "trues," "accidentals," and "dead-time," combined with the monitored rates $(1+2)$, $(2+3)$, (1^*+2), and $(2+3^*)$ enable one to make the first-order corrections for accidental counts and dead-time losses and estimate the higher order corrections to make sure they are negligible. A twenty-channel analyzer gated by the slow coincidence outputs was used to record the output spectrum of the coincidence circuits.
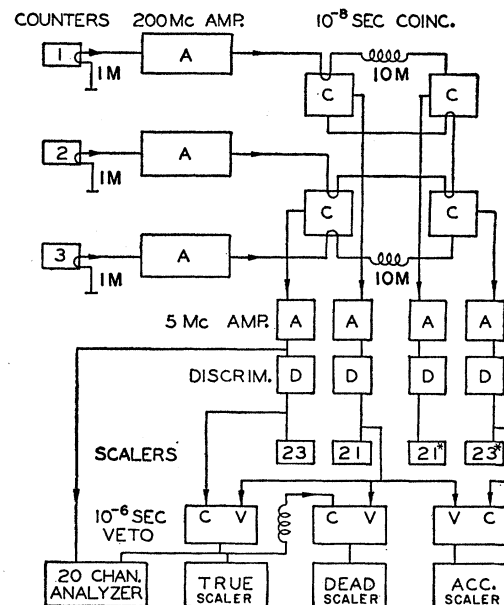

FIG. 2. Block diagram of electronics. The abbreviations are: M, meters of RG114 cable; A, amplifier; C, coincident circuit; D, discriminator; and V, veto circuit.
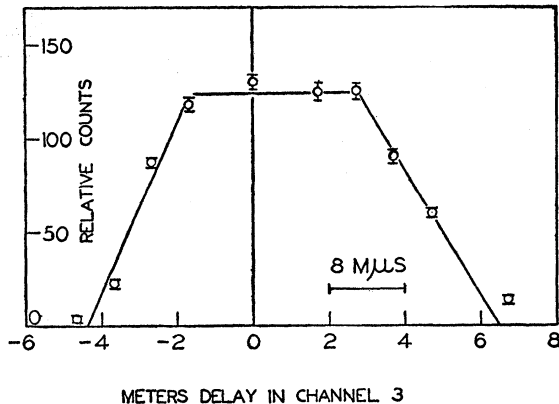
FIG. 3. (2+3) coincidence counting rate as a function of relative delay in channel 3.

III. EXPERIMENTAL PROCEDURE

Preliminary Adjustments

The first step in putting the counting system into operation was to line up the slow amplifiers by observing the output pulse spectrum with the coincidence circuits in self-coincidence. This procedure was subsequently used with a Co γ source in a standard geometry for daily checks on the over-all stability of the system. Delay curves were then run to check the resolving time of the coincidence circuits and the simultaneity of the pulses at the inputs. A typical curve of this type is plotted in Fig. 3 and shows that the resolving time, 2τ, of the coincidence was about 40 mμsec, corresponding to 10 meters delay in channel 3. Finally, the "In-minus-Front" difference was investigated as a function of the voltage on each counter individually and on all counters simultaneously. The plateau obtained for the latter measurement is shown in Fig. 4; the individual plateaus were similar with perhaps slightly less slope.

General Procedure

The experiment was run almost daily for a little over a month and involved an integrated beam energy of 5×10^{16} Mev. Experimental points were obtained for hydrogen and deuterium targets with 300-, 400-, and 500-Mev bremsstrahlung at laboratory angles of 30°, 73°, and 140°. Since changing the gas involved pumping out the target for several hours, the usual procedure at a given angle was to run at all bremsstrahlung energies first with hydrogen, then vacuum, and finally deuterium. This cycle was repeated at least twice and no difficulty was encountered in reproducing runs within the estimated accuracy of ±2% for the gas density determinations and monitor reproducibility. The statistical accuracy of the individual runs was often ±1% or better.

73° and 140° Runs

At 73° and 140°, absorber 1 was 1 in. of Al and absorber 2 was $\frac{3}{4}$ in. of Al. Typical output spectra for the

(2+3) coincidence circuit are shown in Fig. 5. Figure 5(A) shows a pair of consecutive "In" and "Front" runs obtained for a hydrogen target at 73° with 500-Mev bremsstrahlung. Figure 5(B) shows the corresponding runs for an evacuated target. Figure 5(C) shows the associated accidental spectra obtained by introducing an additional 10-meter delay in the lead from counter 3. Such runs will be called "counter 3 delayed runs."

The spectra of Fig. 5 illustrate a number of features of the experiment. The large peak in channels 14 and 15 observed for the hydrogen "In" run is due to neutral particles being converted in the Pb radiator and producing at least one minimum ionizing secondary which traverses both counters 2 and 3. The uniform spectrum of smaller pulses extending down to channel 5, where it has been cut off by a discriminator bias, is due to events in which the energy loss in the counters is less than about one-half minimum. This component, which can also be seen in the hydrogen "Front" run and vacuum runs, was present even when the forward slit was closed with 4 in. of Pb and is therefore associated with a general room background. The exact process occurring was not precisely determined, but evidence that the particles passing between the counters were neutrons was obtained by making absorption measurements in Pb, Cu, and Al.

To obtain the net "In-minus-Front" counting rates, runs were first corrected for small (<1%) counting losses in the scalers. Then accidentals ranging up to 5% were subtracted. These were distributed in pulse height
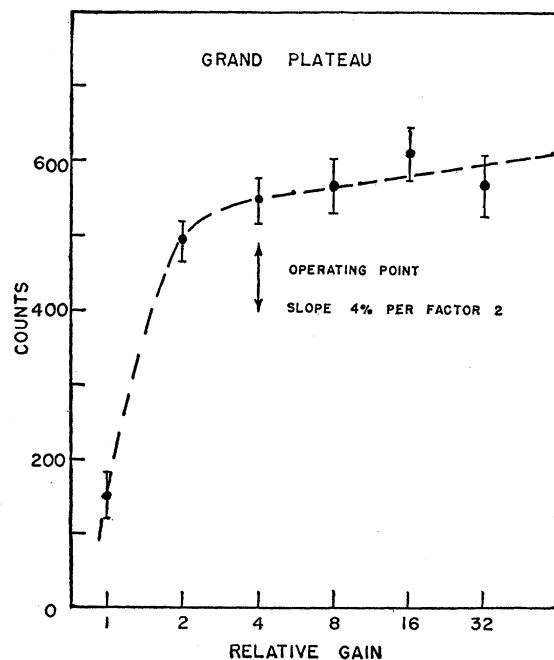

FIG. 4. "In-minus-Front" counting rate as a function of relative gain in all three channels.

and corrected for tracking of the "true" and "accidental" channels using the spectra and ratios of "trues" to "accidentals" obtained in the "counter 3 delayed" runs. The correction for dead-time losses was made by multiplying by the ratio of counts in the "true" and "dead-time" scalers. Dead-time losses rarely exceeded one percent. Next, "In-minus-Front" differences were calculated for corresponding pairs of gas and vacuum runs. These differences were corrected for fluctuations in the monitor sensitivity and normalized to a standard specific volume. The former correction amounted to a maximum of $\pm 1\%$ and could be made with an accuracy of $\pm 50\%$. The latter normalization involved using the equation of state[10] to determine the specific volume of the gas from its measured temperature and pressure and is estimated to be accurate to about $\pm 1.5\%$. Finally, the net counting rate was determined by subtracting the vacuum runs from the gas runs. The result of this procedure applied to the runs shown in Figs. 5(A), 5(B), and 5(C) is shown in 5(D). As can be seen, a very satisfactory subtraction of the small pulses results. In practice a channel by channel reduction was not made for all runs. Rather, the procedure outlined above was carried out for only two groups of pulses: those in the peak, N, and those in the tail, $\Sigma - N$, where Σ is the total number of counts in the spectrum. The net N result was associated with the true counts. A net result close to zero for the $\Sigma - N$ group was obtained in all cases and served as a check on both the experiment and calculations.

30° Runs

At 30° an exceedingly large background of small pulses was encountered. An investigation showed that it was associated with particles entering through the slit, but that it was not due to the gas in the target.
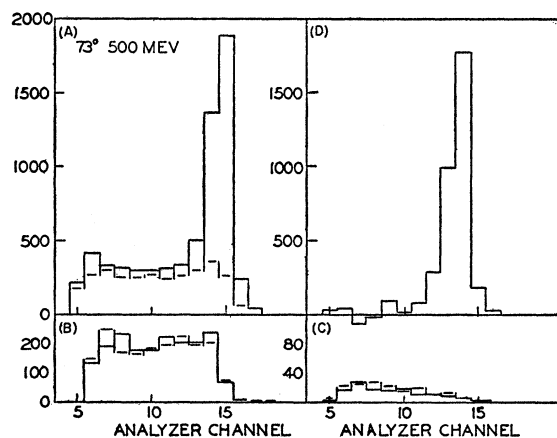

FIG. 5. (A) "In" (solid line) and "Front" (broken line) runs for hydrogen for 73° and 500-Mev bremsstrahlung; (B) corresponding backgrounds for an evacuated target; (C) corresponding accidental spectra obtained by inserting an additional 40 mμsec delay in channel 3; (D) spectrum of net true counts obtained as described in Sec. III.
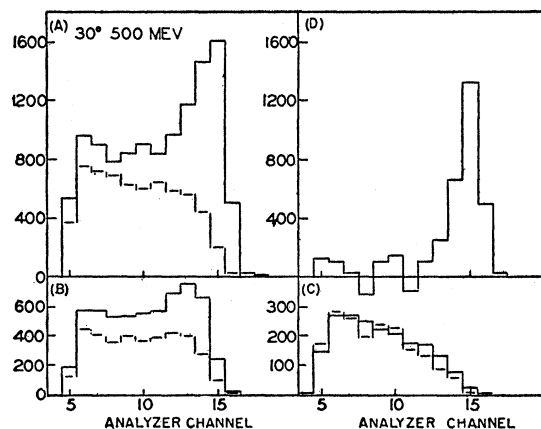

FIG. 6. (A) "In" (solid line) and "Front" (broken line) runs for 30° and 500-Mev bremsstrahlung; (B) corresponding backgrounds for an evacuated target; (C) corresponding accidentals spectra obtained by inserting an additional 40 mμsec delay in channel 3; (D) spectrum of net true counts obtained as described in Sec. III.

Absorption measurements in Pb and Al showed the incident particles to be photons having a mean energy of 5 to 10 Mev and the particles passing between counters 2 and 3 also to be photons with a mean energy of about 5 Mev. One suggestion as to the process occurring was made by Dr. R. Querzoli, who proposed that it might be the double scattering of a single photon which produced to low-energy Compton recoil electrons in the two counters. Although the probability of this process was very small, the single counting rates were so high that if one makes the reasonable assumption that they were due primarily to photons, then it is quite possible to account for the observed background on this basis. Other explanations are also possible. However, since a photon link between counters C_2 and C_3 is involved, the background could have been largely eliminated by requiring a triple, rather than a double, coincidence. Unfortunately, time would not permit us to try this and we were forced to reduce the background to a tolerable level by changing absorber 1 from 1-in. Al to 6-in. CH_2 and increasing absorber 2 from $\frac{3}{4}$-in. to 2-in. Al. Typical $(2+3)$ coincidence spectra for hydrogen, vacuum, and "counter 3 delayed" runs are shown in Figs. 6(A), 6(B), and 6(C), respectively. These runs were analyzed in the manner previously described for the 73° and 140° runs to produce the spectrum in Fig. 6(D). As for the 73° and 140° runs, it was not the usual procedure to make a channel-by-channel analysis, but to analyze only the groups N and $\Sigma - N$. At 30° the $\Sigma - N$ results showed a small positive excess, as seen in Fig. 6(D), which may be associated with soft radiation from electrons scattered into the counter by the gas.

Identification of Particles Counted

The principal evidence that the majority of the counts recorded were photons comes from the fact that (1) they were neutral, since they failed to trigger the veto,

(2) they were converted appropriately in Pb and CH_2, and (3) they were absorbed appropriately in Pb and CH_2. The extent to which we can rule out other particles depends largely on a knowledge of the efficiency of the veto counter, C_1. Although we were unable to devise any simple precise measurement of this efficiency other than running a plateau curve, we know of no reason why it should have been less than 100% for charged particles traversing more than half the counter. Unfortunately, due to lack of forethought, the Pb converter used was larger than the veto counter and therefore the possibility of a net effect in the "In-minus-Front" differences existed due to the slightly different geometry of the two configurations for scattering around the counter. This effect was checked and found to be negligible, however, by cutting out the direct counts with a 4-in. thick Pb plug of just the width of the veto counter, and observing the residual differences. Assuming then that only neutral particles are counted, we conclude that the "In-minus-Front" difference must be due to photons or neutrons converted in the Pb radiator. As can be seen in Table I the Pb radiator is only 3% of the geometrical mean free path for neutrons and the energy of a recoil proton required to trigger the telescope must be greater than 75 Mev for the $\frac{3}{4}$-in. Al absorber 2 used at 73°, and 140 Mev for the 2-in. Al absorber 2 used at 30°. From data on neutron star production in nuclear emulsions,[12] we estimate that not more than a fifth of the interactions caused by 300-Mev neutrons in Pb give protons in this energy range. Since the number of 300-Mev neutrons coming from hydrogen or deuterium will be very small, we can safely assume the neutron counting efficiency to be less than 0.5% while the photon efficiency is in the neighborhood of 50%. Moreover, since the neutron flux from the machine has been found to be comprised of low-energy neutrons, the only high-energy neutrons are the recoils from meson production and deuteron photodissociation and this flux will be of the same magnitude as the photon flux at 30° and much smaller at 73° and 140°. It seems reasonable to assume, therefore, that virtually all the counts recorded in this experiment were due to photons. It should perhaps be pointed out here that even if the efficiency of the veto were less than 100% it would change the "In-minus-Front" differences by a factor which would cancel out in the deuterium-to-hydrogen ratio. This is not true for the usual "In-minus-Out" differences.

IV. RESULTS

Integral Ratios

The ratio of photon yields per nucleon from deuterium and hydrogen are given in Table II-A as a function of bremsstrahlung end point and laboratory angle. The errors shown are the standard deviations due to

[12] Blau, Oliver, and Smith, Phys. Rev. **91**, 949 (1953).

counting statistics and fluctuations in gas density and monitor sensitivity. In addition, there are errors due to fluctuations in the bremsstrahlung end point. These are roughly: ±5% for 300 Mev; ±3% for 400 Mev; and ±5% for 500 Mev and correspond to rms fluctuations in end-point energy of ±1% at 300 and 400 Mev and ±0.5% at 500 Mev.

Difference Ratios

In order to obtain the photon yields associated with bremsstrahlung in an energy interval, $\Delta k = E' - E$, we used the photon difference method. The calculations were based on the following expression for the difference in counting rate, ΔN, between runs with bremsstrahlung end points E' and E:

$$\Delta N = \int_u^{E'} \Gamma(k) N(k,E') dk - \int_u^{E} \Gamma(k) N(k,E) dk \qquad (1a)$$

$$= \int_E^{E'} \Gamma(k) N(k,E') dk$$

$$+ \int_u^{E} \Gamma(k) N(k,E) \left\{ \frac{N(k,E')}{N(k,E)} - 1 \right\} dk, \qquad (1b)$$

where $\Gamma(k)$ is the differential photon yield from bremsstrahlung of energy k, $N(k,E)$ is the number of photons of energy k per unit energy in a bremsstrahlung spectrum of end point E and u is the threshold energy for π^0 production. Since the ratio $N(k,E')/N(k,E)$ is very nearly independent of k, the second integral in Eq. (1b) can be made to vanish by normalizing the runs so that $N(k,E')/N(k,E) \approx 1$. The remaining integral then relates the difference rate, ΔN, to an average value of $\Gamma(k)$ for the interval $\Delta k = E' - E$ which, if Δk is sufficiently small, will be close to $\Gamma(\frac{1}{2}(E'+E))$. A knowledge of $\Gamma(k)$ enables one to deduce differential cross sections for the reaction being studied.

The ratios of difference yield per nucleon for deuterium and hydrogen were computed from the data in Table II-A in accordance with the discussion above and

TABLE II. Part A lists the deuterium-to-hydrogen ratios of photon yield per nucleon as a function of laboratory angle and bremsstrahlung end point. Part B lists the deuterium-to-hydrogen difference-yields per nucleon as a function of laboratory angle and photon energy interval.

θ_2	30°	73°	140°
	A. Integral ratios: $D/2H$		
E(Mev)			
500	0.99±0.02	0.88±0.02	0.91±0.02
400	0.96±0.03	0.91±0.02	0.83±0.04
300	1.25±0.11	0.86±0.04	1.00±0.05
	B. Difference ratios: $\Delta D/2\Delta H$		
ΔE(Mev)			
500–400	1.05±0.14	0.79±0.11	1.70±0.60
400–300	0.86±0.06	0.94±0.05	0.68±0.06
300	1.25±0.11	0.86±0.04	1.00±0.05

are listed in Table II-B as a function of laboratory angle for the energy intervals: threshold to 300 Mev 300 to 400 Mev; and 400 to 500 Mev. The errors given are those deduced from the errors in Table II-A. In addition, there are the errors due to the fluctuations in the bremsstrahlung end point. These errors are greatly magnified by the photon difference method and turn out to be roughly: $\pm 5\%$ for threshold to 300 Mev; $\pm 10\%$ for 300 to 400 Mev; and $\pm 20\%$ for 400 to 500 Mev. The poor control of the bremsstrahlung end point is felt to be the principal known weakness of the present experiment.

V. DISCUSSION OF RESULTS

It was, of course, the object of this experiment to relate the photon yields from deuterium and hydrogen to the cross sections for photoproduction of neutral pions in these elements. In order to do this we must make the assumption that other processes giving secondary photons are negligible. Investigations of the elastic nuclear scattering[7,13,14] indicate that the cross section for this process is less than 2% of the neutral pion cross sections. Since elastic nuclear scattering will tend to cancel in the ratio anyway, it can probably be safely neglected. It is not so obvious, however, that various electronic processes, such as wide-angle bremsstrahlung and pair production and elastic nuclear scattering of electrons, cannot produce secondary photons in competition with neutral pion decay, particularly at 30°. The best evidence that this is at least not too serious comes from experiments similar to this with bremsstrahlung near meson threshold.[7,14] These experiments fail to show any appreciable number of photons from electronic sources and we may assume that, percentage-wise, we should be at least as well off at higher bremsstrahlung energies. If there is a small electronic contribution, it should be the same per *nucleus* for deuterium and hydrogen and would, therefore, tend to make ratios per *nucleon* in Table II too low.

Assuming that all the photons counted result from the decay of neutral pions, the photon counting rate, N, will be related to the center-of-momentum neutral pion cross section, $d\Omega/d\Omega_c$, by the expression:

$$N = N_T \int_u^E \int_\tau \int_\Omega \int_{\Omega_c} \epsilon(k') \frac{d\Omega'}{d\Omega} \frac{d\Omega''}{d\Omega'} \frac{2}{4\pi} \frac{d\sigma}{d\Omega_c}$$
$$\times N(k) d\Omega_c d\Omega d\tau dk, \quad (2)$$

where N_T is the number of nuclei per unit volume of the target; k is the incident photon energy; τ is an element of target volume; Ω is the laboratory solid angle for the decay photons; Ω_c is the center-of-momentum solid angle for the neutral pions; $N(k)$ is the number of photons per unit energy in the bremsstrahlung; $2/4\pi$ is

[13] D. C. Oakley and R. L. Walker, Phys. Rev. 97, 1297 (1955); Ernstene, Keck, and Tollestrup (private communication).

[14] F. E. Mills, University of Illinois thesis, 1955 (unpublished).

the number of decay photons per unit solid angle in the pion rest system; $d\Omega''/d\Omega'$ is the solid-angle transformation which carries the decay photons from the pion rest system to center-of-momentum system; $d\Omega'/d\Omega$ is the solid angle transformation which carries the decay photons from the center-of-momentum system to the laboratory system; $\epsilon(k')$ is the efficiency of the photon detector as a function of photon energy, k'; u is the threshold energy for neutral pion production; and E is the bremsstrahlung end point.

All of the quantities appearing in the integral can be expressed as functions of the variables of integration (see Appendix A). If the solid angle of the photon counter, Ω, is sufficiently small, the integral may be factored and the integration over the target volume and solid angle carried out. This gives the expression

$$N = N_T C \int_u^E N(k) \int_{\Omega_c} 2\epsilon(k') \frac{d\Omega'}{d\Omega} \frac{d\Omega''}{d\Omega'} \frac{d\sigma}{d\Omega_c} \frac{d\Omega_c}{4\pi} dk, \quad (3)$$

where C is a constant of the geometry (see Appendix A). This expression shows that the measured yields are related to the neutral pion cross sections in quite a complicated manner, so that the ratio of photon counts for deuterium and hydrogen will be equal to the ratio of neutral-pion cross sections only if all the factors in the integral have the same form for the two cases. Equation (3) can be made to take on a simpler form if we note that the factor

$$\Theta(k,\theta_c) = \frac{1}{\epsilon_\pi(k)} \int_0^{2\pi} 2\epsilon(k') \frac{d\Omega'}{d\Omega} \frac{d\Omega''}{d\Omega'} \frac{d\varphi_c}{4\pi} \sin\theta_c, \quad (4)$$

implied in Eq. (3) is the effective angular resolution of the system for detecting neutral pions. The normalizing factor $\epsilon_\pi(k)$ is the average efficiency for detecting neutral pions produced by photons of energy k for a fixed laboratory angle of observation and is defined by the equation

$$\epsilon_\pi(k) = \int_{\Omega_c} 2\epsilon(k') \frac{d\Omega'}{d\Omega} \frac{d\Omega''}{d\Omega'} \frac{d\Omega_c}{4\pi}. \quad (5)$$

Introducing definitions (4) and (5) into Eq. (3), we obtain

$$N = N_T C \int_u^E N(k) \epsilon_\pi(k) \int_0^\pi \Theta(k,\theta_c) \frac{d\sigma}{d\Omega_c} d\theta_c. \quad (6)$$

The angular resolution function $\Theta(k,\theta_c)$ can be evaluated analytically if $\epsilon(k')$ is constant and numerically if $\epsilon(k')$ is known (see Appendix A). Plots of $\Theta(k,\theta_c)$ for constant $\epsilon(k')$ are shown in Fig. 7 for a photon energy of 330 Mev and laboratory angles of 30°, 73°, and 140°.

The situation becomes somewhat simpler if we integrate the photon flux over all laboratory angles. In
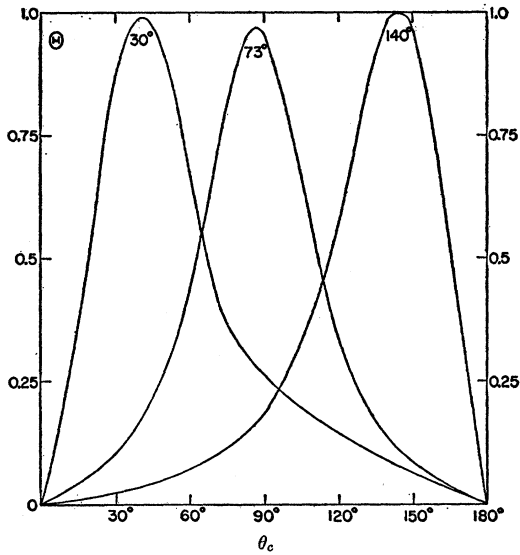
FIG. 7. Effective resolution functions Θ for pions produced by 330-Mev photons for the three angles of observation employed ($\theta = 30°$, $73°$, and $140°$).

this case, we obtain from Eq. (2)

$$I \equiv \int_\Omega N d\Omega = N_T \int_u^E N(k) \epsilon_\gamma(k) \sigma_T dk, \tag{7}$$

where $\epsilon_\gamma(k)$ is the average efficiency for detecting neutral pions produced by photons of energy k in a fixed direction in the center-of-momentum system and is defined by the equation

$$\epsilon_\gamma(k) = \int_\Omega 2\epsilon(k') \frac{d\Omega'}{d\Omega'} \frac{d\Omega''}{d\Omega} \frac{d\Omega}{4\pi}. \tag{8}$$

Note that $\epsilon_\gamma(k)$ is independent of θ_c and is not in general equal to $\epsilon_\pi(k)$.

At the present time, the efficiency $\epsilon(k')$ of the photon counter is not known in detail. Qualitative arguments, however, lead one to expect that, over the range of decay photon energies most heavily weighted in the above integrals, it was probably constant. More important than an assumption concerning the efficiency is the additional assumption we wish to make that the motion of the nucleons within the deuteron does not distort the dynamics of the decay photons sufficiently to affect the average efficiencies $\epsilon_\pi(k)$ and $\epsilon_\gamma(k)$ which appear in expression (6) and (7). This point has not been investigated in detail, but it is difficult to believe that the effect could be important for most of the momenta encountered in the deuteron.

The discussion above has been given to make clear in detail just how the data in Table II are related to the neutral-pion cross sections. We shall now make the simple assumption, previously mentioned, that the constant C and the form of the integrands in Eqs. (6)

and (7) are the same for deuterium and hydrogen and proceed to equate the ratio of photons to the ratio of neutral pions. Some support for this is given by the fact that, at least for 73° and 140°, the ratios listed in Table II are all consistent with a constant value of 0.9 per nucleon. It should be borne in mind that difference data in Table II-B are correlated in such a way that a systematic error in an entry in Table II-A which results in a high difference ratio in one energy interval will also result in a low ratio in an adjacent interval. Some of the scatter in the ratios in Table II-B is probably due to this effect, (see 300- to 400-Mev and 400- to 500-Mev intervals at 140°). At 30° there may be an indication of somewhat larger ratios than 0.9, particularly for the threshold-to-300-Mev interval. Such an increase at forward angles and low photon energies would be predicted on the basis of the impulse approximation[15] if the amplitudes for production of neutral pions on the proton and neutron interfered constructively. A quantitative fit with the theory was not attempted, however, due to the uncertainty of the data and the difficulty of unfolding the complicated angular resolution. The qualitative evidence obtained here supports already existing evidence obtained by direct observations of the elastic photoproduction of neutral pions in deuterium[16] that the interference is indeed constructive and hence the coupling of neutral pions to protons and neutrons is opposite in sign, as expected for the "symmetrical meson theory."

Returning to the ratio of 0.9 per nucleon observed at 73° and 140°, we note that this value is in good agreement with that reported by Cocconi and Silverman.[7] They made observations similar to ours for 300-Mev bremsstrahlung and found ratios accurate to about 10%, which scatter about an average value of 0.9 and give no particular evidence of a variation with angle from 45° to 150°. Measurements have also been made as a function of pion energy at 90° by Andre[6] who used the $\gamma - \gamma$ coincidence method. His values group around 1.2 with errors of 25 to 50% and are therefore not in disagreement with a value of 0.9. However, in the forward direction the interference effects within the deuteron should be appreciable. A calculation of the total cross section for π^0 production was made on the basis of the impulse approximation. These calculations indicate that the integral ratio at 500 Mev and 30° should be 1.4 compared to the measured value of 0.99 and at 500 Mev and 90°, 1.15 compared to the observed value of 0.88. Chappelear[17] has considered the effects of multiple scattering within the deuteron on the elastic π^0 cross section and has shown that the coherent

[15] G. F. Chew and H. W. Lewis, Phys. Rev. 84, 779 (1951); N. C. Francis and R. E. Marshak, Phys. Rev. 85, 496 (1952); Heckrotte, Henrich, and Lepore, Phys. Rev. 85, 490 (1952); N. C. Francis, Phys. Rev. 89, 766 (1953).
[16] Wolfe, Silverman, and Dewire, Phys. Rev. 99, 268 (1955); H. L. Davis and D. R. Corson, Phys. Rev. 99, 273 (1955); J. W. Rosengren and N. Baron, Phys. Rev. 101, 410 (1956).
[17] J. Chappelear, Phys. Rev. 99, 254 (1955).

interference effects are considerably suppressed. It is possible that these same effects are responsible for the suppression of the total cross section noted above.

If we assume, on the basis of the constant value of the ratio at large angles, that interference effects in the deuteron are negligible except at small angles and low photon energies, it follows that the cross section for photoproduction of neutral pions in the deuteron should be the sum of those for the proton and neutron.[15]

The authors wish to acknowledge the help and support of all the members of the synchrotron laboratory. They wish to thank particularly Dr. R. F. Bacher for his encouragement of the work, and Dr. R. V. Langmuir, Dr. R. Querzoli, Dr. M. Sands, Dr. J. G. Teasdale, Dr. R. L. Walker, and Mr. B. H. Rule for assistance in running the synchrotron.

APPENDIX A

The following expressions relate the quantities in the integral in Eq. (2), Sec. V to the variables of integration:

$$d\Omega''/d\Omega' = (1-\beta_\pi{}^2)/(1-\beta_\pi \cos\alpha)^2, \tag{A1}$$

$$d\Omega'/d\Omega = (1-\beta_c{}^2)/(1-\beta_c \cos\theta)^2, \tag{A2}$$

$$\gamma = \frac{\mu c^2}{2}\left\{\frac{(1-\beta_\pi{}^2)^{\frac{1}{2}}}{(1-\beta_\pi \cos\alpha)}\frac{(1-\beta_c{}^2)^{\frac{1}{2}}}{(1-\beta_c \cos\theta)}\right\}, \tag{A3}$$

$$\beta_\pi = \left\{1-\left(1+\frac{2k}{M}\right)\Big/\left(\frac{k}{\mu}+\frac{\mu}{2M}\right)^2\right\}^{\frac{1}{2}}, \tag{A4}$$

$$\beta_c = 1/[1+(M/k)], \tag{A5}$$

$$\cos\alpha = \sin\theta' \sin\theta_c \cos\phi_c + \cos\theta' \cos\theta_c, \tag{A6}$$

$$\cos\theta' = (\cos\theta - \beta_c)/(1-\beta_c \cos\theta), \tag{A7}$$

where β_c is the velocity of the center-of-momentum of the incident photon, k, and the target proton, M; β_π is the velocity of the neutral pion of mass μ in the center-
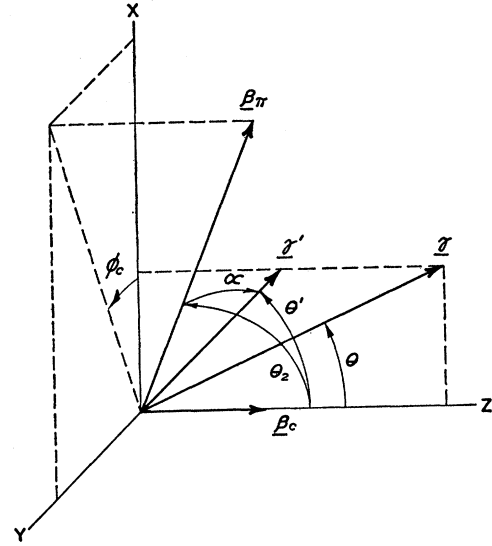

FIG. 8. Angles involved in transforming the neutral pion decay photons to the laboratory system. In the center of the figure, "θ_z" should read "θ_c."

of-momentum system, and γ is the energy of a decay photon in the laboratory system. The angles are those shown in Fig. 8, where γ' is the momentum of the decay photon in the center-of-momentum system.

For the geometry used in this experiment the constant, C, in Eq. (3), Sec. V is given by:

$$C = \frac{ah\omega}{lc \sin\theta}(1+\alpha+\cdots), \tag{A8}$$

where a is the width of the Pb slit, h is the height of counter 2, ω is the width of counter 2, l is the distance from counter 2 to the slit, and C is the distance from counter 2 to the point where the axis of the telescope intersects the axis of the beam. α is a correction term which is <0.005.